Movement of rice yellow mottle virus between xylem cells through pit membranes

NATACHA OPALKA*†, CHRISTOPHE BRUGIDOU*, CAROLINE BONNEAU*, MICHEL NICOLE‡, ROGER N. BEACHY*†, MARK YEAGER§¶, AND CLAUDE FAUQUET*

*International Laboratory for Tropical Agricultural Biotechnology (ILTAB/ORSTOM-TSRI), †Division of Plant Biology, and §Department of Cell Biology, The Scripps Research Institute (TSRI), BCC 206, 10550 North Torrey Pines Road, La Jolla, CA 92037; and ‡ORSTOM (Institut Francais de Recherche Scientifique pour le Développement en Coopération), Laboratoire de Phytopathologie, BP 5045, 34032 Montpellier, France

ABSTRACT   The translocation of rice yellow mottle virus (RYMV) within tissues of inoculated and systemically infected *Oryza sativa* L. leaves was characterized by Western immunoblotting, Northern blotting, and electron microscopy of thin sections. In inoculated leaves, RYMV RNA and coat protein first were detected at 3 and 5 days postinoculation, respectively. By 6 days postinoculation, RYMV had spread systemically to leaves, and virus particles were observed in most cell types, including epidermal, mesophyll, bundle sheath, and vascular parenchyma cells. Most of the virions accumulated in large crystalline patches in xylem parenchyma cells and sieve elements. Colocalization of a cell wall marker for cellulosic β-(1–4)-D-glucans and anti-RYMV antibodies over vessel pit membranes suggests a pathway for virus migration between vessels. We propose that the partial digestion of pit membranes resulting from programmed cell death may permit virus migration through them, concomitant with autolysis. In addition, displacement of the Ca^{2+} from pit membranes to virus particles may contribute to the disruption of the pit membranes and facilitate systemic virus transport.

To achieve systemic infection, plant viruses move from cell to cell and over long distances by exploiting the transport mechanisms for macromolecules within the host plant. It is now well-established for a range of plant viruses that cell-to-cell movement of a viral genome through plasmodesmata is mediated by movement proteins (MPs) (see refs. 1–3 for recent reviews). Certain MPs interact with elements of the cytoskeleton and other cellular structures that may be involved in intracellular and intercellular movement (4–6). Interestingly, MPs of plant viruses such as cowpea mosaic virus participate in cell-to-cell transport by inducing the formation of tubular structures through which virions can pass (7).

Less is known about the translocation of viruses throughout the plant than is known about local, cell-to-cell movement. To achieve long-distance movement, plant viruses enter the vascular system (phloem and/or xylem), move within, and exit the vasculature at some distal point. However, the mechanisms of loading and unloading of viruses within conducting elements (sieve tubes and xylem vessels) and their migration to surrounding cells is poorly understood. The flow of metabolites within conducting elements influences the movement of plant viruses (8), and it is accepted that the movement of viruses through the phloem follows the flow of photoassimilate from source to sink leaves (9). Recently it was shown that phloem transport of soluble carboxyfluorescein and potato virus X was similar, including the unloading of both solute and virus from minor veins (10). Long-distance movement involves different

mechanisms than those involved in movement between mesophyll cells, and in a number of cases, efficient movement through the vascular system requires virus assembly (11–14). In addition, for tobacco etch virus, distinct domains in the coat protein (CP) are involved in cell-to-cell and long-distance movement (15). Although many viruses have been documented to move long distances through the phloem, few viruses have been reported to move in the xylem (16, 17). Among the sobemoviruses, blueberry shoestring virus and southern bean mosaic virus were reported to move in both phloem and xylem tissues (18–21).

Rice yellow mottle virus (RYMV), a member of the sobemovirus genus, causes substantial economic losses in rice production from eastern to western Africa (22, 23). Infected plants typically exhibit yellowing and discoloration of the leaves and stunting and are sterile. RYMV is an icosahedral virus of 25–28 nm in diameter (24) and is naturally transmitted by chrysomelid beetles (22, 25). Its genome is composed of a single-stranded positive-sense RNA of 4,450 nucleotides containing four ORFs (26). Frame-shift and deletion mutations introduced in the CP cistron in an infectious cDNA clone demonstrated that the CP was not required for RNA replication, but was necessary for long-distance and possibly cell-to-cell spread of infection (27). Previous histological studies on thin sections of infected rice leaves demonstrated the presence of RYMV in the epidermis, mesophyll, and mestome sheath cells (24). However, it is not known whether RYMV is transported in the xylem or the phloem or both. To elucidate the mechanism of long-distance movement of RYMV, we performed ultrastructural and cytochemical studies in infected *Oryza sativa* plants.

MATERIALS AND METHODS

Virus Isolation and Inoculation of Plants. The RYMV isolate used in this study was collected from rice fields in the Ivory Coast. The virus was propagated in rice (*O. sativa* L.), variety IR8 and was purified as described previously (27).

Protein Extraction and Western Immunoblot Analysis. Proteins were extracted from rice leaves of three plants per sample (28) in 1 vol of 2× loading buffer (29). Thirty micrograms of total protein was separated on 12.5% polyacrylamide gels containing SDS. Western immunoblotting was performed with a polyclonal antibody raised against purified RYMV as described previously (27). Analyses were performed on inoculated leaves from 1 to 5 days postinoculation (dpi) and on systemically infected leaves from 6 to 28 dpi. After 5 dpi,

inoculated leaves were yellow and dried and could not be sampled.

RNA Extraction and Northern Blot Analysis. Total RNA was extracted from inoculated leaves (1, 2, 3, and 5 dpi) and systemically infected leaves (6, 14, 21, and 28 dpi) (30). Equivalent amounts of total RNA (15 μg) were denatured and fractionated on 1.2% agarose gels containing formaldehyde (31). RNAs were transferred by blotting to Hybond N⁺ membranes (Amersham). Prehybridization and hybridization were carried out with a DNA probe corresponding to ORF1 of RYMV-RNA nucleotides 80–553 (26, 27). The DNA probe was obtained by PCR amplification by using primers 5'-dGCATCGTGTATGACACGGTT-3' (nucleotides 70–90) and 5'-dCAGGACTGATTCTCTCAAAA-3' (nucleotides 547–567) and was purified by using Geneclean (Bio 101). DNA was labeled by random primer labeling (Stratagene) and purified by Nuctrap push columns (Stratagene). The membranes were washed at 65°C twice with 2× SSC (standard saline citrate), 0.1% SDS for 10 min, twice with 1× SSC, 0.1% SDS for 15 min, and once with 0.1× SSC, 0.1% SDS for 15 min.

Tissue Preparation for Ultrastructural Studies. Inoculated leaves were harvested at 2, 3, and 5 dpi, and systemic leaves at 7, 10, 14, 17, 21, and 28 dpi. Roots were harvested from 2 to 28 dpi. Samples were fixed for 2 h in 1.5% (vol/vol) glutaraldehyde and 4% paraformaldehyde (vol/vol) in 0.1 M cacodylate buffer at pH 7.4, rinsed in cacodylate buffer (3 × 20 min), and postfixed for 1 h in 1% (vol/vol) osmium tetroxide. After three 30-min washes in cacodylate buffer, leaf and root fragments were progressively dehydrated in a 10% graded series of 0–100% ethanol and then in propylene oxide for 1 h. Samples were embedded in Epon (Taab Laboratories Equipment, Reading, United Kingdom), and thin sections were stained with uranyl acetate and lead citrate and then examined by transmission electron microscopy in a Philips CM12 operating at 100 kV. For each time point (dpi), observations were made on 20 sections from three different resin blocks. Purified virus also was embedded in Epon resin as control.

Tissue Preparation for Immunolabeling Studies. For immunolocalization of RYMV particles, samples were dehydrated in ethanol as noted above and embedded in London Resin White resin (Taab). Sections were labeled on grids by using anti-RYMV polyclonal antibodies followed by goat anti-rabbit gold conjugate (GAR10, Biocell Laboratories) (32). After staining with saturated uranyl acetate and lead citrate (10 min each), the grids were examined by electron microscopy as described above. Specificity of labeling was assessed by comparing infected and noninfected leaves and incubation with preimmune serum in place of the primary antiserum. The density of labeling (D) was calculated by determining the number of gold particles per μm² ± SE. Ten to 15 micrographs were taken from three different blocks from infected and noninfected rice leaves (21 dpi).

Cytolocalization of β-(1–4)-D-Glucans. To confirm the localization of RYMV particles over vessel pit membranes, an exoglucanase complexed with 20 nm colloidal gold particles was used to identify β-(1–4)-D-glucans from cellulose according to the method of Benhamou (33).

RESULTS

Time Course of CP and Viral RNA Accumulation in Infected *O. sativa* Plants. By Western blot analysis, RYMV-CP was detected in inoculated leaves at 5 dpi (Fig. 1*A*). In systemically infected leaves, RYMV-CP was detected at 6 dpi and continued to accumulate over the time of the experiment (Fig. 1*A*). By Northern blot analysis, a weak band of hybridization corresponding to the genome length viral RNA (4,450 nucleotides) was detected at 3 dpi in inoculated leaves (Fig. 1*B*, 3I) and over the next 2 days, there was a dramatic increase in the level of RNA (Fig. 1*B*, 5I). At 6 dpi, the viral hybridization

A

B
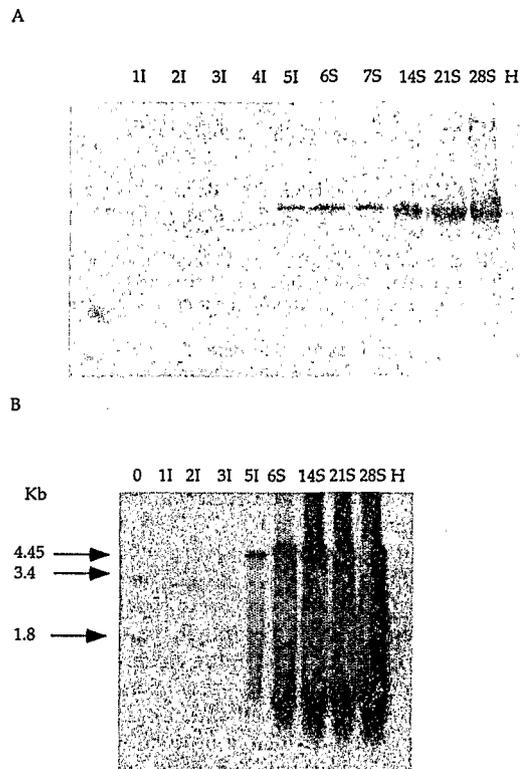
FIG. 1. Detection of RYMV protein and RNA during the time course of infection of rice leaves. Numbers above the lanes refer to dpi. H, uninfected control; I, inoculated leaves; S, systemically infected leaves. (*A*) Western immunoblot analysis of the CP. (*B*) Northern blot analysis. Arrows identify the bands corresponding to RYMV genomic RNA (4.45 kb), 25S ribosomal RNA (3.4 kb), and 17S RNA (1.8 kb), respectively (34, 35).

signal was detected in systemically infected leaves and was present up to 28 dpi (Fig. 1*B*). These results indicate that systemic infection by RYMV occurs within 6 dpi, during which viral RNA and CP accumulate.

Distribution of RYMV in Infected Plants. Inoculated and systemically infected leaves were examined by electron microscopy of thin sections. In inoculated leaves, virus particles were not detected from 1 to 5 dpi. In systemically infected leaves, the distribution of virus particles was sporadic at 10 dpi in xylem and bundle sheath tissues (data not shown). At 14 dpi, most of the virus particles were observed in vascular tissues. Within xylem parenchyma cells, virus particles were densely packed in vacuoles and in the cytoplasm (Fig. 2*A*). In xylem vessels, virions were closely associated with pit membranes, between vessels and pit membranes adjacent to parenchyma cells, as well as in secondary walls. Occasionally, virus particles were detected in the vacuoles and the cytoplasm of phloem parenchyma cells (data not shown). After 14 dpi, large quantities of virions were dispersed in vessel elements (Fig. 2*B*), accumulating in paracrystalline arrays in vacuoles of parenchyma cells and in vessels associated with pit membranes (Fig. 3 *A–C*). These crystals were not seen in healthy tissues, and no particles were observed associated with pit membranes (Fig. 3*D* and *E*). At 21 dpi, crystals of virus particles also were observed in sieve elements of phloem (data not shown). These results suggest that RYMV can move over long distances through xylem and phloem and gain access to the vascular parenchyma cells of systemically infected leaves.

Examination of bundle sheath cells revealed dispersed virus particles in vacuoles (data not shown). In mesophyll cells of plants at 14 dpi, electron-dense material was detected in nuclei, within cytoplasm, and within vacuoles (Fig. 4 *A* and *B*). Virus-like particles also were identified within the plasmod-

FIG. 2. Infected xylem tissue in 14-dpi plants. (*A*) This infected xylem parenchyma cell contains virus particles in a vacuole (Va) and in the cytoplasm (thick arrow). Note also the presence of virus particles in a vessel (V) close to a pit membrane between two vessels (P), a pit membrane associated with the parenchyma cell (Pa) and close to the secondary walls (S) (thin arrows). (*B*) An infected vessel with virus particles. (Bars = 500 nm.)

FIG. 3. Infected xylem tissue in 21-dpi plants. (*A*) A paracrystalline region of virus particles (C) displays angled edges and striations spaced at 26 nm, consistent with the regular crystalline packing of virus particles. This crystal can be distinguished from the adjacent, amorphous noncrystalline aggregate (A). Note the presence of particles against the pit membrane and the secondary wall (thick arrows). (*B*) A close-up view of the paracrystalline array (*Left*) and the amorphous material (*Right*). (*C*) Pit membrane (P) with secondary wall (S) between two vessels with associated virus particles. (*D*) Uninfected parenchyma cell. (*E*) Noninfected pit membrane with a loose arrangement of microfibrils. [Bars = 1 μm (*A* and *C*) and 0.5 μm (*B*, *D*, and *E*).]

esmata connecting mesophyll cells (Fig. 4*C*). In addition, chloroplast membranes in infected tissues occasionally formed finger-like extrusions (Fig. 4*D*). These morphological changes were not observed in control noninfected plants (Fig. 4*E*). At 21 dpi, virions accumulated in epidermal cells and in guard cells with no apparent cytological changes (data not shown). These results show that RYMV is not restricted to the xylem and the phloem tissues and can move to the epidermis. In contrast, roots contained very few RYMV particles at 21 dpi, and particles were limited to vascular tissues (data not shown).

Detection of RYMV Particles by Immunogold Labeling. Polyclonal anti-RYMV antibodies were used to confirm the accumulation of virus within infected tissues. No significant labeling was observed over the electron-dense material in the cytoplasm (data not shown). In infected xylem tissue from 21-dpi plants, gold particles were closely associated with virus particles over pit membranes between vessels (Fig. 5*A*). In contrast, healthy xylem tissue showed no significant labeling (Fig. 5*B*). Labeling also was detected over virus particles located in the vessel lumen and pit membranes associated with parenchyma cells (Fig. 5*C*). Quantitation of gold particles indicated that significant labeling occurred over pit membranes between vessels, vessel secondary cell walls, and the

lumens of virus-filled vessels, whereas pit membranes adjacent to parenchyma cells were labeled to a much lower degree (Table 1). In this study, all veins of systemically infected leaves that were examined showed extensive labeling over virus particles in vessels.

Cytolocalization of β-(1–4)-D-Glucans. To confirm the localization of virus particles within vessel pit membranes, an exoglucanase-gold complex was used to locate β-(1–4)-D-glucans in infected and noninfected tissues. Pit membranes as well as secondary walls were evenly labeled in infected and noninfected leaves (Fig. 5*D*). Over vessel cell walls of infected tissues, gold particles associated with cellulose were distributed close to virus particles that were free of labeling (Fig. 5*D*). To assess the specificity of the reaction, samples were preincubated with a β-(1–4)-D-glucans derived from barley: this treatment prevented antibody labeling (data not shown).

DISCUSSION

In this study of RYMV in infected rice leaves, we examined the accumulation of viral RNA and CP and the distribution of virus particles in tissues of inoculated and systemically infected *O. sativa* L. leaves by Western immunoblotting, Northern blotting, and electron microscopy of thin sections. Viral RNA first was detected in inoculated leaves at 3 dpi, and by 6 dpi, RYMV had spread to systemically infected leaves. CP was
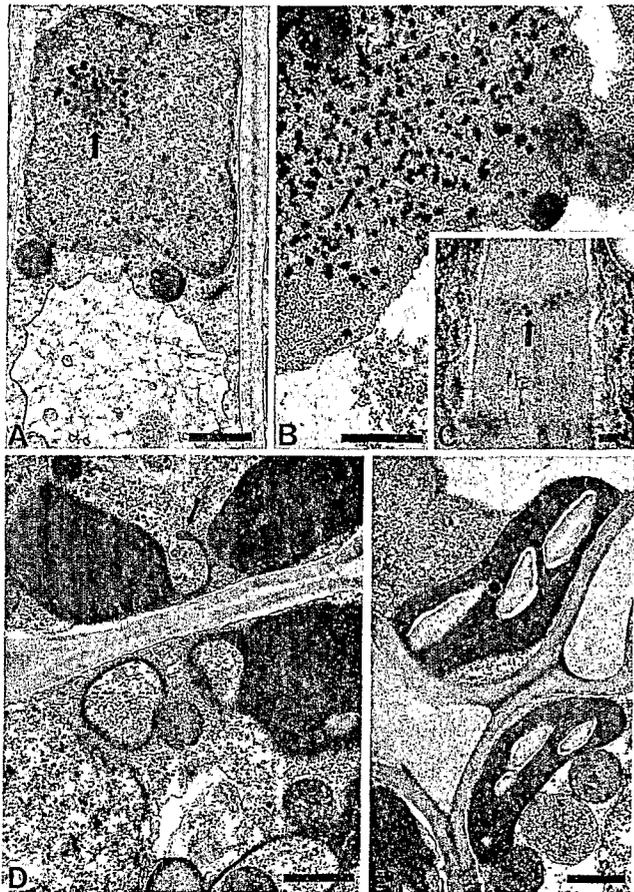
FIG. 4. Infected mesophyll cells in 14-dpi plants. (*A* and *B*) Electron-dense material in a nucleus and in the cytoplasm (thick arrows) (bars = 1 μm). (*C*) Virus-like particles in plasmodesmata (thick arrow) (bar = 100 nm). (*D*) Chloroplasts in infected cells display finger-like membrane extrusions (thin arrow) (bar = 1 μm). (*E*) Uninfected mesophyll cell with well-defined chloroplasts and regular stacking of the thylakoid membranes. (Bar = 1 μm.)

detected at 5 dpi in inoculated leaves and accumulated to higher levels in systemically infected leaves. The similarities in patterns of accumulation of RNA and CP are consistent with the observation that RYMV-CP is essential for systemic infection (27).

Virion Assembly May Be Required for Systemic Infection. At the early stages of infection, we did not observe virus particles in inoculated leaves. In contrast, the presence of virions in systemically infected leaves indicates that encapsidation may be required for long-distance transport. The failure of systemic spread of another sobemovirus, southern bean mosaic virus C, in a resistant host was related to the absence of virion formation (36). Similar observations also have been reported for other plant viruses, including tobacco mosaic virus and red clover necrotic mosaic virus (3, 13, 14).

Accumulation of RYMV in Vascular Tissues. In this study, we observed the accumulation of large amounts of RYMV in xylem parenchyma cells and vessels. Because upward movement of solutes primarily occurs in the xylem rather than phloem, the predominant localization of RYMV within xylem implies that the upward flow pattern through xylem facilitates the systemic spread of infection. It previously was suggested that southern bean mosaic virus (18) and potato mop-top virus (37) are transported in xylem vessels to allow their spread throughout the plant. Primary xylem tissues also may be important sites for the multiplication of RYMV, as is suggested by the presence of large aggregates of virus in xylem parenchyma cells. RYMV particles were observed to a lesser
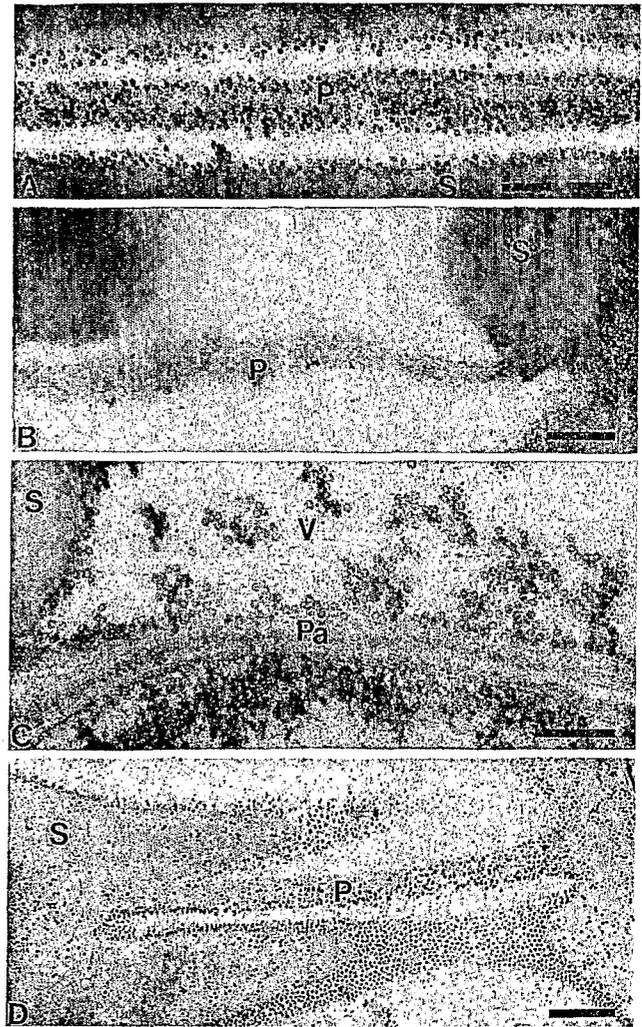
FIG. 5. Immunodetection of RYMV (*A–C*) and cytolocalization of β-1,4-D-glucans (*D*) in 21-dpi plants. (*A*) Gold particles associated with virus particles over pit membranes (P) (bar = 500 nm). (*B*) No significant labeling was detected in uninfected tissue (bar = 200 nm). (*C*) Labeling over virus particles dispersed in the vessel and close to the pit membrane associated with a parenchyma cell (Pa) (bar = 200 nm). (*D*) Dense labeling over the vessel secondary cell walls (S) and the pit membrane (P) between two vessels (V) (bar = 500 nm). Control experiments using preimmune serum showed no significant labeling (data not shown).

extent in phloem sieve elements. Transport from these conducting elements to neighboring cells, if it occurs, likely takes place via plasmodesmata that connect the conducting element to an adjacent cell. Plasmodesmata that are converted into sieve pores in the end walls between adjacent sieve elements also may provide a route for virus transport. Only a few viruses have been reported to follow a similar pathway in long-distance transport. Examples include maracuja mosaic virus, which was observed in vascular parenchyma cells and in vessel elements

Table 1.   Density of gold particles obtained with anti-RYMV antibodies over pit membranes in healthy and infected xylem tissues

	Healthy tissue*	Infected tissue*
Vessel pit membrane	2.88 ± 2.58	183.77 ± 142.21
Vessel pit membrane associated to a parenchyma cell	0.40 ± 0.32	58.33 ± 18.69
Vessel secondary wall	0.03 ± 0.09	128.39 ± 82.860
Vessel lumen	0.45 ± 0.80	177.89 ± 110.154
Vessel background	0	2.94 ± 3.020

*Gold particles per μm² ± SE.

Plant Biology: Opalka *et al.*

Proc. Natl. Acad. Sci. USA 95 (1998)   3327
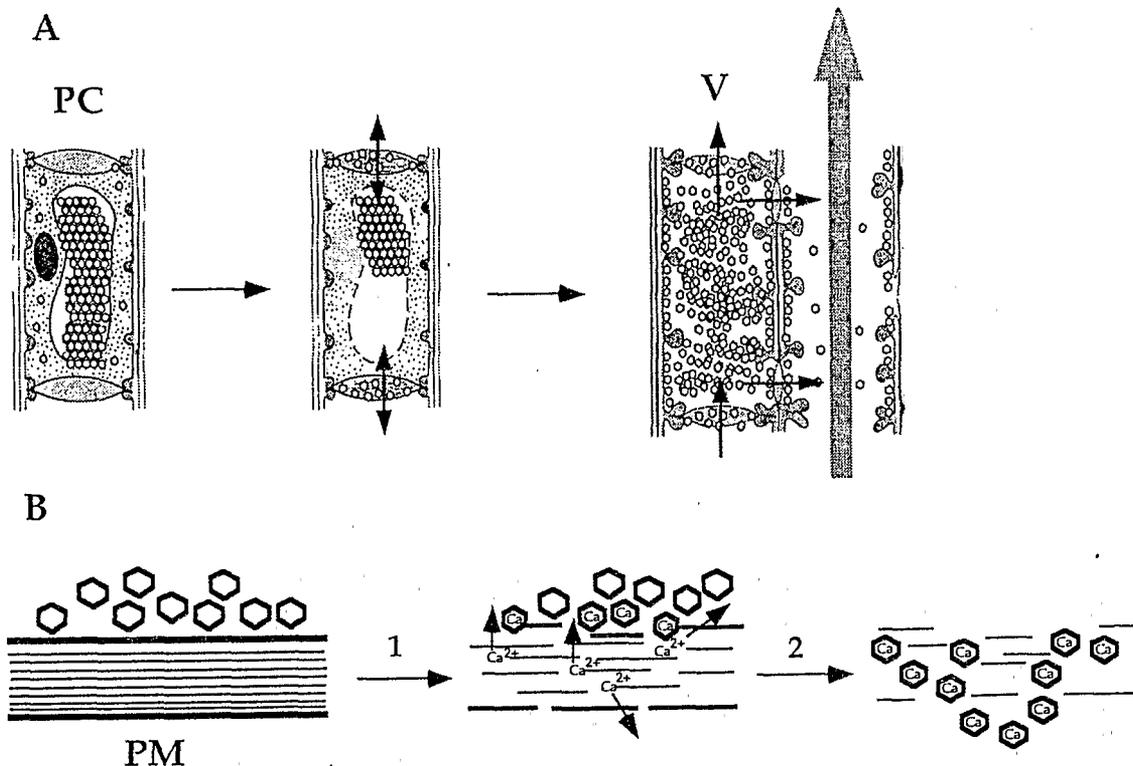
FIG. 6.   Model for the cell-to-cell movement of RYMV in xylem. (*A*) During the differentiation of parenchyma cells (PC) to vascular elements (V) cells undergo programmed cell death, which results in the loss of cellular contents. In this process, virus particles (v) are passively transported to vessels. (*B*) During the maturation of xylem, intervascular pit membranes (PM) are disrupted as a consequence of programmed cell death. We suggest that chelation of pit membrane calcium by virus particles exacerbates the dissolution of the pit membranes and propose that such disruption enables the transport of virions between vessels.

(38), and barley yellow striate mosaic virus, which was detected in conducting elements of phloem and in xylem (39).

RYMV Infection Is Associated with Multiple Cytopathological Effects. After long-distance movement, RYMV spreads from infected vascular elements to mesophyll cells. Although the significance of the dense amorphous material within the nucleus and the cytoplasm is not known, such structures also have been detected in cells infected by wheat streak mosaic rhimovirus and tomato spotted wilt tospovirus (40, 41). The accumulation of large numbers of virus particles suggests that virus replication occurs in these cells. RYMV-like particles were observed within plasmodesmata between mesophyll cells, indicating that cell-to-cell spread in these tissues is via virions. It is well known that some plant viruses can move via modified plasmodesmata as virions (42–44). Structural modifications of plasmodesmata have been reported in virus-infected tissues, including increases in size and absence of the desmotubule, and may indicate transport of virions (2).

A Model for the Translocation of RYMV in Xylem. This study demonstrated that large amounts of RYMV accumulated in xylem elements as well as in parenchyma cells. We suggest that this accumulation occurs as a consequence of infection of xylem parenchyma cells, resulting in virus replication and virus accumulation. Subsequently, these cells undergo programmed cell death that leads to the formation of mature tracheary elements, i.e., the conducting elements (vessels) (45). It has been reported that in rice plants the differentiation of vessels can occur when the leaf is fully expanded (46). As a result, virions may be transported throughout the plant in these elements along with solute. In addition to the accumulation of virions in mature xylem cells, we observed close association of RYMV with intervascular pit membranes; these structural elements separate adjacent cells that are in the process of differentiation and are composed of

primary cell walls and a middle lamella. During the differentiation of vessels, hydrolysis of intervascular pit membranes appears to begin in the middle lamella in poplar (47) and cultured *Zinnia* cells (48). In addition, the partial digestion of primary walls of pit membranes during differentiation leads to a loose arrangement of microfibrils, which may favor virus translocation, as was suggested for southern bean mosaic virus (18) and beet necrotic yellow vein virus (49). The pit membranes appear to be less compact in infected compared with noninfected tissues and may be structurally altered by the infection. We propose that the pit membranes, which are maintained by Ca^{2+}-pectin polymers that comprise the middle lamella, are disrupted by the virus (Fig. 6). It is known that structural integrity of the capsid shell of sobemoviruses is dependent on the chelation of Mg^{2+} and Ca^{2+} (50). We propose that during the process of hydrolysis of the pit membrane, virus particles bind the Ca^{2+} from the membrane, thereby stabilizing the capsid shells, and further disrupting the pit membrane. In this model the passage of virions through pit membranes would be an active process involving ionic interactions between the pit membrane and the virions. Whether or not a similar mechanism is responsible for transport of virus between a vessel and a living parenchyma cell remains to be examined.

1. Citovsky, V. & Zambryski, P. (1991) *BioEssays* **13**, 373–379.
2. Maule, A. J. (1991) *Crit. Rev. Plant Sci.* **9**, 457–473.
3. Carrington, J. C., Kasschau, K. D., Mahajan, S. K. & Schaad, M. C. (1996) *Plant Cell* **8**, 1669–1681.
4. Heinlein, M., Epel, B. L., Padgett, H. S. & Beachy, R. N. (1995) *Science* **270**, 1983–1985.
5. McLean, B. G., Zupan, J. & Zambryski, P. C. (1995) *Plant Cell* **7**, 2101–2114.
6. Gilbertson, R. L. & Lucas, W. J. (1996) *Trends Plant Sci.* **1**, 260–268.
7. van Lent, J., Storms, M., van der Meer, F., Wellink, J. & Goldbach, R. (1991) *J. Gen. Virol.* **72**, 2615–2623.
8. Bennett, C. W. (1940) *J. Agric. Res.* **60**, 361–390.
9. Leisner, S. M., Turgeon, R. & Howell, S. H. (1993) *Plant Cell* **5**, 191–202.
10. Roberts, A. G., Santa Cruz, S., Roberts, I. M., Prior, D. A. M., Turgeon, R. & Oparka, K. J. (1997) *Plant Cell* **9**, 1381–1396.
11. Siegel, A., Zaitlin, M. & Sehgal, O. P. (1962) *Proc. Natl. Acad. Sci. USA* **48**, 1845–1851.
12. Dawson, W. O., Bubrick, P. & Grantham, G. L. (1988) *Phytopathology* **78**, 783–789.
13. Saito, T., Yamana, K. & Okada, Y. (1990) *Virology* **176**, 329–336.
14. Vaewhongs, A. A. & Lommel, S. A. (1995) *Virology* **212**, 607–613.
15. Dolja, V. V., Haldeman, R., Robertson, N. L., Dougherty, W. G. & Carrington, J. C. (1994) *EMBO J.* **13**, 1482–1491.
16. Chambers, T. C. & Francki, R. I. B. (1966) *Virology* **29**, 673–676.
17. Cruz, F. C. S. & Koganezawa, H. (1991) *Int. Rice Res. Newsl.* **16**, 14.
18. Schneider, I. R. & Worley, J. F. (1959) *Virology* **8**, 230–242.
19. Schneider, I. R. & Worley, J. F. (1959) *Virology* **8**, 243–249.
20. Weintraub, M. & Ragetli, H. W. J. (1970) *J. Ultrastruct. Res.* **32**, 167–189.
21. Urban, L. A., Ramsdell, D. C., Klomparens, K. L., Lynch, T. & Hancock, J. F. (1989) *Phytopathology* **79**, 488–493.
22. Bakker, W. (1970) *Netherlands J. Plant Pathol.* **76**, 53–63.
23. Awoderu, V. A. (1991) *J. Basic Microbiol.* **31**, 91–99.
24. Bakker, W. (1974) Ph.D. thesis (Agricultural University, The Netherlands).
25. Bakker, W. (1971) *Netherlands J. Plant Pathol.* **77**, 201–206.
26. Ngon a Yassi, M., Ritzenthaler, C., Brugidou, C., Fauquet, C. & Beachy, R. N. (1994) *J. Gen. Virol.* **75**, 249–257.
27. Brugidou, C., Holt, C., Ngon a Yassi, M., Zhang, S., Beachy, R. N. & Fauquet, C. (1995) *Virology* **206**, 108–115.
28. Sandstrom, R. P., Deboer, A. H., Lomax, T. L. & Cleland, R. E. (1987) *Plant Physiol.* **85**, 693–698.
29. Laemmli, U. K. (1970) *Nature (London)* **227**, 680–685.
30. Carrington, J. C. & Morris, T. J. (1984) *Virology* **139**, 22–31.
31. Gerard, F. G. & Miller, K. (1986) *Focus* **8**, 5–6.
32. Pietschmann, S. M., Hausmann, E. H. S. & Gelderblom, H. R. (1989) in *Colloidal Gold: Principle, Methods and Applications*, ed. Hayat, M. A. (Academic, New York), Vol. 2, pp. 256–284.
33. Benhamou, N. (1989) *Electron Microsc. Rev.* **2**, 123–138.
34. Takaiwa, F., Oono, K. & Sugiura, M. (1984) *Nucleic Acids Res.* **12**, 5441–5448.
35. Sugiura, M., Iida, Y., Oono, K. & Takaiwa, F. (1985) *Gene* **37**, 255–259.
36. Fuentes, A. L. & Hamilton, R. I. (1993) *J. Gen. Virol.* **74**, 1903–1910.
37. Jones, R. A. C. (1975) *Phytopathol. Z.* **82**, 352–355.
38. Fribourg, C. E., Koenig, R. & Lesemann, D. E. (1987) *Phytopathology* **77**, 486–491.
39. Robertson, N. L. & Carroll, T. W. (1989) *J. Ultrastruct. Mol. Struct. Res.* **102**, 139–146.
40. Urban, L. A., Hang, P.-Y. & Moyer, J. W. (1991) *Phytopathology* **81**, 525–529.
41. Gao, J. G. & Nassuth, A. (1993) *Phytopathology* **83**, 206–213.
42. De Zoeten, G. A. & Gaard, G. (1969) *J. Cell Biol.* **40**, 814–823.
43. Kitajima, E. W., Lauritis, J. A. (1969) *Virology* **37**, 681–685.
44. Robards, A. W. & Lucas, W. J. (1990) *Annu. Rev. Plant Physiol. Plant. Mol. Biol.* **41**, 369–419.
45. Pennell, R. I. & Lamb, C. (1997) *Plant Cell* **9**, 1157–1168.
46. Miyake, H. & Maeda, E. (1976) *Ann. Bot.* **40**, 1131–1138.
47. Benayoun, J. (1983) *Ann. Bot.* **52**, 189–200.
48. Burgess, J. & Linstead, P. (1984) *Planta* **160**, 481–489.
49. Dubois, F., Sangwan, R. S. & Sangwan-Norreel, B. S. (1994) *Protoplasma* **179**, 72–82.
50. Hsu, C. H, Sehgal, O. P. & Pickett, E. E. (1976) *Virology* **69**, 587–595.

ISSN = 0027-8424

NEWTON
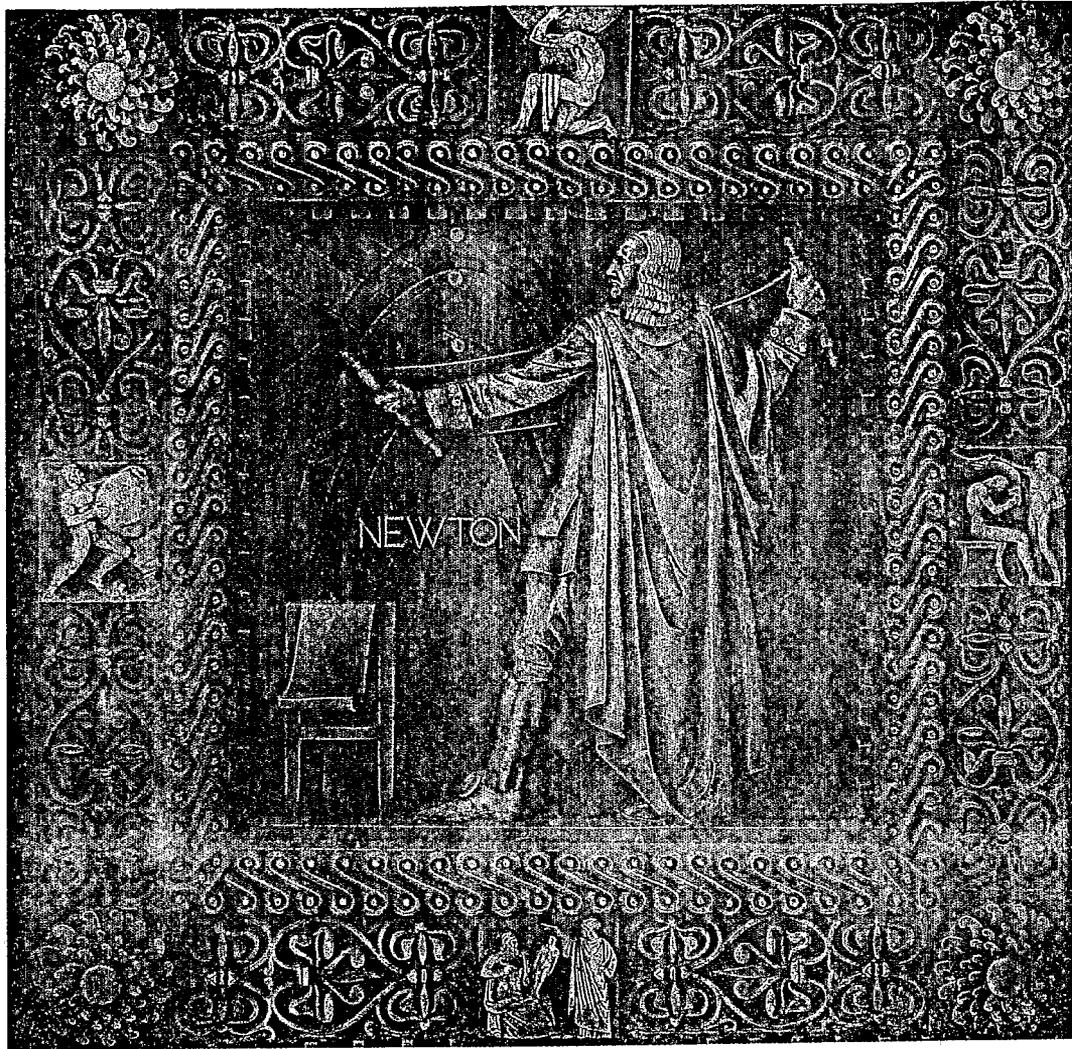
PROCEEDINGS

OF THE

NATIONAL ACADEMY OF SCIENCES

OF THE UNITED STATES OF AMERICA